A pressurized model for compressible pipe flow.

Mehmet Ersoy

A pressurized model for compressible pipe flow.

M. Ersoy*[1]

[1]Université de Toulon, IMATH, EA 2134, 83957 La Garde, France.

Abstract

We present the full derivation of a compressible model in a thin closed water pipe including friction, changes of section and slope variation. Starting from the compressible 3D Navier-Stokes equation under "thin layer" assumptions with well-suited boundary conditions, we justify the 1D reduced model called pressurized model (also named the **P**-model). It was introduced in the general framework of unsteady mixed flows in closed water pipes. This model describes the evolution of a compressible flow close to gas dynamics equations in a nozzle. We also propose a class of averaged low Oser compressible models of a general barotropic law $p(\rho) = \rho^\gamma$, $\gamma > 1$.

Keywords: pressurized flow, compressible Navier-Stokes, barotropic laws, thin layer, hydrostatic approximation, closed water pipe, friction, viscosity, Oser number
AMS Subject classification : 65M08, 65M75, 76B07, 76M12, 76M28, 76N15

1 Introduction

Simulation of pressurized flows (i.e. the pipe is full) as well as free surface (i.e. only a part of the pipe is filled) in closed water pipe plays an important role in many engineering applications such as storm sewers, waste or supply pipes in hydroelectric installations .... The transition phenomenon between the two types of flows occurs in many situations and it can be induced by sudden change in the boundary conditions as failure pumping. During this process, in particular for pressurized flows, the pressure can reach severe values and may cause irreversible damage. Accurate mathematical and numerical models are required to predict and to avoid such a situation.

From a numerical viewpoint, the use of the full 3D Navier-Stokes equations lead to time-consuming simulations. Introducing reduced models preserving some of the main physical features is one of the most challenging issues that we address with the obvious consequence to decrease the computational time. During these last years, a great amount of works was devoted to the modeling and the simulation of such a phenomenon (see for instance [18, 25, 24, 10, 9, 16], [8, 3, 2, 11, 4, 5] and the reference therein).

The classical shallow water equations, commonly used to describe free surface flows in open channels, are also used in the study of pressurized flows with the artifice of the Preissman (see for example [9, 28]) assuming a narrow slot to exist in the upper part of the pipe. The width of the slot is calibrated to provide the correct sonic speed. Nevertheless, as pointed out by several authors (see [25] for instance), the pressurizing phenomenon is a dynamic shock requiring a full dynamic treatment even if the inflows and other boundary conditions change slowly. Moreover, the Preissman slot artefact is unable to take into account the depressurisation phenomenon (i.e. sub-atmospheric flows) which occurs during a water hammer. On the other hand the commonly used model to describe pressurized flows in closed water pipes are the Allievi equations which are derived by neglecting some acceleration terms. As a consequence, the resulting first order system is not written under a conservative form and thus it is not well adapted to a natural

*Mehmet.Ersoy@univ-tln.fr

coupling with a shallow water model which describes the evolution of free surface flows in closed water pipes. Thus, the pressurized model was formally introduced by the author in [11, 5] as an extension of the work by Bourdarias and Gerbi [8]. The obtained 1D equations for pressurized flows was derived from the 3D isentropic compressible Euler equations to take into account sub-atmospheric flows with a formulation closed to the Saint-Venant equations for free surface flows. As a consequence, the free surface model and the pressurized model was coupled to construct a "unified" model for unsteady mixed water flows. The formal derivation of this model, called **PFS**-model (see [11, 5]), as well as a finite volume discretization have been previously proposed by Bourdarias and Gerbi [8]. This works was extended by the author [5] in the case of non uniform section and a new VFRoe solver [3] as well as a new kinetic solver [2, 4] have been proposed.

Although, all of these models was formally derived, numerical experiment versus laboratory experiment was presented [3, 2, 4]) and the proposed schemes for the **P**-model, as well as for the **PFS**-model, produce results that are in a very good agreement. Under the hypothesis

$$u \approx \overline{u} \quad \text{and} \quad \overline{\rho u} \approx \overline{\rho}\ \overline{u}$$

the **P**-model is an accurate approximation of the Euler equations in a "thin-layer" framework. The so-called pressurized model is:

$$\left\{ \begin{array}{lcl} \partial_t A + \partial_x Q & = & 0, \\ \partial_t Q + \partial_x \left(\dfrac{Q^2}{A} + c^2 (A - S) \right) & = & -gA \sin\theta + c^2 \left(\dfrac{A}{S} - 1 \right) \dfrac{d\,S}{dx} \end{array} \right. \tag{1}$$

where $\overline{\rho}$ is the mean density of the water, $A = \overline{\rho} S$ is the equivalent wet area, $\overline{u}$ is the mean water velocity, $Q = A\overline{u}$ is the equivalent discharge, S is the section of the pipe, c is the sonic speed and $\sin\theta$ is the "slope variation". To take into account the friction, a quadratic term $-\rho g C_f u|u|$ was added to the system (1). The friction factor C_f is defined by

$$C_f = \frac{1}{K_s^2 R_h(S(x))^{4/3}}\ ,$$

where K_s is the Strickler coefficient of roughness depending on the material, $R_h(S) = S/P_m$ is the hydraulic radius and P_m is the perimeter of the pipe's section.

We propose here to justify the pressurized model as an approximation at order $O(\varepsilon)$ of the full 3D compressible Navier-Stokes system where ε is the aspect ratio assumed to be small

$$\varepsilon = \frac{D}{L} \ll 1\ ,$$

as recently done by Ersoy [12] for the 3D-1D reduced free surface model in open channel and closed water pipe. In particular, we show that the "motion by slices" assumption,

$$u \approx \overline{u} \quad \text{and} \quad \overline{\rho u} \approx \overline{\rho}\ \overline{u}$$

used to formally derive the pressurized model, are exact at first order and

$$u = \overline{u} + O(\varepsilon),\ \overline{\rho u} = \overline{\rho}\ \overline{u} + O(\varepsilon)\ .$$

These results are obtained with well suited boundary conditions including friction and the pressure law is chosen as a linear one $p(\rho) = c^2(\rho - \rho_0)$. It allows to take into account sub-atmospheric and sup-atmospheric flows where ρ_0 stands for the density of the water at atmospheric pressure.

Moreover, assuming that the Oser number, the ratio between the Mach number and the Froude number, is small, we derive a class of averaged compressible models in a closed water pipe with a general pressure law $p(\rho) = \rho^\gamma$ for $\gamma > 1$. In particular, we show that at first order

$$\overline{\rho^\gamma} = \overline{\rho}^\gamma$$

which is wrong in general if the Oser number is not small enough.

The paper is organized as follows. In Section 2, we recall the compressible Navier-Stokes equations with suitable boundary conditions including friction and we fix the notations. In Section 3, we first deduce the so-called motion by slices and other assumptions required to derive the pressurized model under thin-layer assumptions from the hydrostatic approximation of the compressible Navier-Stokes equations. Then, these equations are integrated following the section orthogonal to the main flow direction and the 1D pressurized model is obtained. Finally, we end with Section 4 where we discuss about a class of averaged low Oser compressible models in a thin-layer domain.

2 The compressible Navier-Stokes equations and its closure

In this section, we fix the notations of the geometrical quantities involved to describe the thin closed domain representing a pipe. Then, we recall the compressible Navier-Stokes system written in the Cartesian coordinates with a gravity. We define the wall-law boundary conditions to include a general friction law completed with a no penetration condition. For the sake of simplicity, we do not deal with the deformation of the domain induced by the change of pressure. For the case of deformation of the pipe due to the change of pressure, we refer to the work by Bourdarias and Gerbi [8] where a Hooke's law is used. We will consider only an infinitely rigid pipe with circular sections.

2.1 Notations and settings

Let us consider a compressible fluid confined in a three dimensional domain $\mathcal{P}$, a pipe of length L oriented following the $\mathbf{i}$ vector,

$$\mathcal{P} := \big\{(x,y,z) \in \mathbb{R}^3;\ x \in [0,L],\ (y,z) \in \Omega(x)\big\}$$

where the section $\Omega(x)$, $x \in [0,L]$, is

$$\Omega(x) = \{(y,z) \in \mathbb{R}^2;\, y \in [\alpha(x,z), \beta(x,z)],\ z \in [-R(x), R(x)]\}$$

as displayed on figure 1(a).

The main flow direction is supposed to be in the $\mathbf{i}$ direction. Thus the section $\Omega(x)$, $x \in [0,L]$, is assumed to be orthogonal to the main flow direction.

Here $R(x)$ stands for the radius of the pipe section $S(x) = \pi R^2(x)$, $\alpha(x,z)$ (resp. $\beta(x,z)$) is the left (resp. the right) boundary point at elevation $-R(x) \leqslant z \leqslant R(x)$.

In the Ω-plane, we define the coordinate of a point $\mathbf{m} \in \partial\Omega(x)$, $x \in [0,L]$, by $(y, \varphi(x,y))$ where $\varphi(x,y) = \sqrt{R(x)^2 - y^2}$ for $y > 0$ and $\varphi(x,y) = -\sqrt{R(x)^2 - y^2}$ for $y < 0$. The point $\mathbf{m}$ stands for the vector $\omega\mathbf{m}$ where $w(x,0,b(x))$ defines the main slope elevation of the pipe with $b'(x) = \sin\theta(x)$. Then, we note $\mathbf{n} = \dfrac{\mathbf{m}}{|\mathbf{m}|}$ the outward unit vector at the point $\mathbf{m} \in \partial\Omega(x)$, $x \in [0,L]$ as represented on figure 1(b).

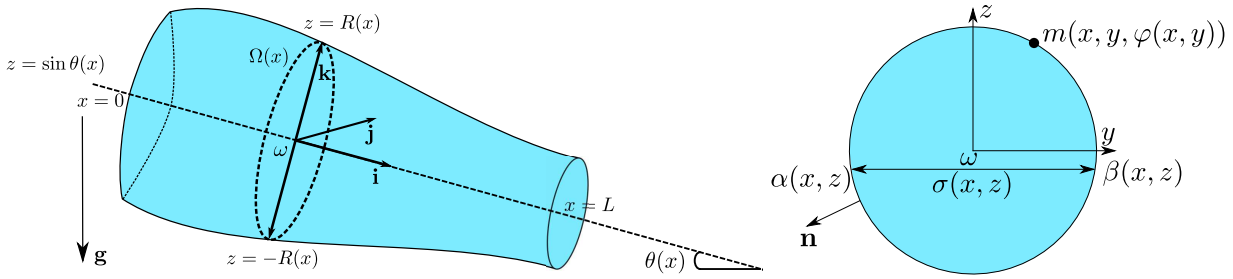

(a) Configuration (b) Ω-plane

Figure 1: Geometric characteristics of the pipe

Remark 2.1. For the sake of simplicity, we consider here only pipe with circular section. This work can be easily adapted to all type of realistic pipe by defining appropriately $R(x)$ and other quantities involved in the definition of the geometry of the pipe (see [11]). For instance, in case of "horseshoe" section as shown in figure 2, the section $\Omega(x)$, $x \in [0, L]$, is given by

$$\Omega(x) = \Omega_H(x) \cap \Omega_R(x)$$

where

$$\Omega_H(x) = \left\{(y, z) \in \mathbb{R}^2; y \in [\alpha(x, z), \beta(x, z)],\ z \in [-H(x), 0]\right\}$$

and

$$\Omega_R(x) = \{(y, z) \in \mathbb{R}^2;\ y \in [\alpha(x, z), \beta(x, z)],\ z \in [0, R(x)]\}\ .$$

H is the height of the trapezoidal basis and R is the radius of the upper part of the "horseshoe".

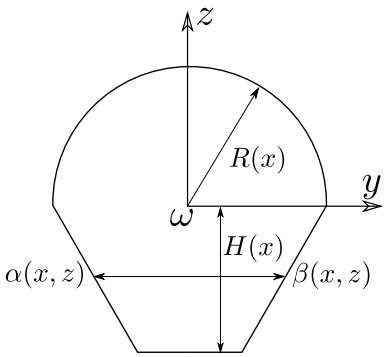

Figure 2: "horseshoe" section

Remark 2.2. For the sake of simplicity, the pressurized model is derived here in the Cartesian coordinates instead of the original one [5]. In the original work, the compressible Euler equations was written in a local Serret-Frenet frame attached to the main pipe axis in order to take into account the local effects produced by the changes of section and the slope variation. This approach introduces naturally a curvature term in the derivation. Thus, as a minor difference, this term will not be present in this framework.

2.2 The compressible Navier-Stokes model

We consider the compressible Navier-Stokes equations in the domain $\mathcal{P}$ with suitable boundary conditions on the inner wall and inflows/outflows conditions at the upstream and downstream ends. The governing equations for the motion of a compressible fluid in $[0, T] \times \mathcal{P}$, $T > 0$ are given by

$$\left\{\begin{array}{rcl} \partial_t \rho + \mathrm{div}(\rho \mathbf{u}) & = & 0\ , \\ \partial_t(\rho \mathbf{u}) + \mathrm{div}(\rho \mathbf{u} \otimes \mathbf{u}) - \mathrm{div}\sigma - \rho F & = & 0\ , \\ p & = & p(\rho)\ , \end{array}\right. \tag{2}$$

where $\mathbf{u} = \begin{pmatrix} u \\ \mathbf{v} \end{pmatrix}$ is the velocity fields with u the $\mathbf{i}$-component and $\mathbf{v} = \begin{pmatrix} v \\ w \end{pmatrix}$ the Ω-component, ρ is the density of the fluid and $F = g \begin{pmatrix} \sin\theta(x) \\ 0 \\ -\cos\theta(x) \end{pmatrix}$ is the external gravity force.

The Cauchy stress tensor is given by

$$\sigma = \begin{pmatrix} -p + \lambda \mathrm{div}(\mathbf{u}) + 2\mu\partial_x u & R(\mathbf{u})^t \\ R(\mathbf{u}) & -pI_2 + \lambda \mathrm{div}(\mathbf{u}) I_2 + 2\mu D_{y,z}(\mathbf{v}) \end{pmatrix} \tag{3}$$

where I_2 is the identity matrix, μ is the dynamical viscosity and $R(\mathbf{u})$ is defined by $R(\mathbf{u}) = \mu\left(\nabla_{y,z}u + \partial_x \mathbf{v}\right)$. Here, $\nabla_{y,z}u = \begin{pmatrix} \partial_y u \\ \partial_z u \end{pmatrix}$ is the gradient of u with respect to (y,z). Noting $\cdot^t$ the transpose of $\cdot$, we define the strain tensor $D_{y,z}(\mathbf{v})$ with respect to the variable (y,z):

$$2D_{y,z}(\mathbf{u}) = \nabla_{y,z}\mathbf{v} + \nabla^t_{y,z}\mathbf{v}\ .$$

The last term $\lambda \mathrm{div}(\mathbf{u})$ is the classical normal stress tensor which plays an important role when the fluid is rapidly compressed or expanded, such as in shock waves. The quantity λ is the volume viscosity, often called second viscosity, is usually assumed to be of the same order of magnitude as the dynamical viscosity μ (see [20]).

Remark 2.3. In the literature, there exists several approach to define the stress tensor in order to set a privileged flow direction.
For incompressible fluids, one has for instance,

- Gerbeau and Perthame [17] use an isotropic stress tensor with constant viscosity to derive the Saint-Venant equations from the 2D incompressible Navier-Stokes equations,
- Marche [21] or Ferrari and Saleri [15], in a similar way, derive a two dimensional shallow water equations from the 3D incompressible Navier-Stokes equations.

In the case of compressible fluids, Ersoy *et al* [14, 13] (based on the work by Kochin [19]) use the following anisotropic total stress tensor:

$$\sigma = -pI_3 + 2\Sigma.D(u) + \lambda \mathrm{div}(u)\, I_3$$

to set a privileged horizontal flow direction in the context of atmosphere modeling. The term $\Sigma.D(u)$ is defined as:

$$\begin{pmatrix} 2\mu D_x(\mathbf{u}) & \mu_2 R(\mathbf{u})^t \\ \mu_3 R(\mathbf{u}) & 2\mu_3 \partial_y v \end{pmatrix}$$

where I_3 is the identity matrix and $\Sigma = \Sigma(t,x,y)$ is the anisotropic viscous tensor:

$$\begin{pmatrix} \mu(t,x,y) & \mu(t,x,y) & \mu_2(t,x,y) \\ \mu(t,x,y) & \mu(t,x,y) & \mu_2(t,x,y) \\ \mu_3(t,x,y) & \mu_3(t,x,y) & \mu_3(t,x,y) \end{pmatrix}.$$

In their case, they obtain a viscous hydrostatic approximation called Compressible Primitive Equations.

In no instance, up to our knowledge, there are now works (except the free surface model by Ersoy [12]) which justify a 1D model from a 3D model in a thin-layer framework.

Finally, the pressure law is given by the following equation of state:

$$p(\rho) = c^2\rho \tag{4}$$

where c is the sonic speed.

Remark 2.4. In practice, $c = \dfrac{1}{\sqrt{\beta_0\rho_0}} \approx 1400\, m^2/s$ where $\beta_0 \approx 5.0\, 10^{-10}\, m^2/N$ is the inverse of the bulk modulus of compression of the water and ρ_0 is the volumetric mass of water.

Remark 2.5. In practical applications, we set

$$p(\rho) = p_a + c^2(\rho - \rho_0)$$

which has the advantage to show clearly overpressure state and depression state. Indeed, the overpressure state corresponds to $\rho > \rho_0$ while $\rho < \rho_0$ represents a depression state. The case $\rho = \rho_0$ is a critic one and a bifurcation point in the context of unsteady mixed flows (see [11, 5] for further details).

2.3 The boundary conditions

The Navier-Stokes system (2)–(4) is completed with suitable boundary conditions to introduce the border friction term. For pipe flow calculations, the Darcy-Weisbach equation, valid for laminar as well as turbulent flows, is generally adopted while the Manning formula is widely used for open channel (in turbulent regime). This factor C_f depends upon several parameter such as the Reynolds number, the relative roughness, ... Because of the extreme complexity of the rough surfaces of mean length δ, most of the advances in understanding have been developed around experiments leading to charts such as the Moody-Stanton diagram, expressing C_f as a function of the Reynolds number R_e, the relative roughness and some geometrical parameters depending on the material. Several formula such as Colebrook formula, Manning, Chézy, Swamee and Jain... have been introduced to represents natural pipe trends. For large Reynolds number, the friction factor C_f is almost function of the relative roughness $\dfrac{\delta}{D_h}$ where D_h is the hydraulic diameter. More precisely, one can show from the Colebrook law that $C_f = C_t + \dfrac{C_l}{R_e}$ where C_l, C_t are some quantity depending on the relative roughness $\dfrac{\delta}{D_h}$ and hydraulic parameters of the pipe. As a consequence if the relative roughness is negligible, the friction factor can be expressed only in function of the Reynolds number. We refer to [26, 28] for more details.

Thus, on the inner wall $\partial\Omega(x)$, $\forall x \in (0, L)$, we assume a wall-law condition including a general friction law:

$$(\sigma(\mathbf{u})n_b) \cdot \tau_{b_i} = (\rho k(\mathbf{u})\mathbf{u}) \cdot \tau_{b_i}, \;\; x \in (0, L), \;\; (y, z) \in \partial\Omega(x)$$

where $k(\mathbf{u}) = C_f|\mathbf{u}|$ and C_f is the friction factor depending on the material. The vector τ_{b_i} is the i^{th} vector of the tangential basis.

Let us detail the wall-law boundary conditions for the sake of completeness. Let us first write this condition as follows:

$$\sigma(\mathbf{u})n_b - (\sigma(\mathbf{u})n_b \cdot n_b)\, n_b = \rho k(\mathbf{u})\mathbf{u}, \;\; x \in (0, L), \;\; (y, z) \in \partial\Omega(x) \; .$$

Here n_b stands for the unit outward normal vector:

$$n_b = \frac{1}{\sqrt{(\partial_x\varphi)^2 + \mathbf{n} \cdot \mathbf{n}}} \begin{pmatrix} -\partial_x\varphi \\ \mathbf{n} \end{pmatrix}$$

where $\mathbf{n} = \begin{pmatrix} -\partial_y\varphi \\ 1 \end{pmatrix}$ is the outward normal vector in the Ω-plane. Thus, the wall-law boundary conditions are written:

$$R(\mathbf{u}) \cdot \mathbf{n} \; (\mathbf{n} \cdot \mathbf{n} - (\partial_x\varphi)^2) + 2\mu\partial_x\varphi \, (D_{y,z}(\mathbf{v})\mathbf{n} \cdot \mathbf{n} - \partial_x u \; (\mathbf{n} \cdot \mathbf{n})) = \left(\mathbf{n} \cdot \mathbf{n} + (\partial_x\varphi)^2\right)^{3/2} \rho k(u)u \; , \tag{5}$$

$$2\mu(\partial_x\varphi)^2 \, (D_{y,z}(\mathbf{v})\mathbf{n} - \mathbf{n}) + \partial_x\varphi R(\mathbf{u}) \; (\mathbf{n} \cdot \mathbf{n} - (\partial_x\varphi)^2) = \left(\mathbf{n} \cdot \mathbf{n} + (\partial_x\varphi)^2\right)^{3/2} \rho k(\mathbf{v})\mathbf{v} \; . \tag{6}$$

We complete it with a no-penetration condition:

$$\mathbf{u} \cdot n_b = 0, \;\; x \in (0, L), \;\; (y, z) \in \partial\Omega(x)$$

i.e.

$$u\partial_x\varphi = \mathbf{v} \cdot \mathbf{n}, \;\; x \in (0, L), \;\; (y, z) \in \partial\Omega(x) \; . \tag{7}$$

3 The averaged model

In a thin-layer domain, the flow follows the main pipe axis and thus it is almost unidirectional. For instance, in the supply pipes in hydroelectric installations, pipes are such that the average thickness D is small in front of the characteristic length L. Besides the fact that the aspect ratio is small

$$\varepsilon = \frac{D}{L} \ll 1 \; ,$$

we should assume that the characteristic speed in the Ω-plane $\boldsymbol{V} = (V, W)$ is small compared to the horizontal one U:

$$\frac{W}{U} \approx \frac{V}{U} \ll 1$$

in order to get a unidirectional flow. These physical considerations define the so-called "thin-layer" assumptions.

3.1 The adimensionnalised Navier-Stokes equations

Thus, in the sequel we adimensionnalise the Navier-Stokes system using the "thin-layer" assumptions by introducing a "small" parameter

$$\varepsilon = \frac{D}{L} = \frac{W}{U} = \frac{V}{U} \ll 1.$$

We then introduce a characteristic time T such that $T = \dfrac{L}{U}$ and we note ρ_0 a characteristic density of the water. The dimensionless quantities of time $\tilde{t}$, coordinate $(\tilde{x}, \tilde{y}, \tilde{z})$, velocity field $(\tilde{u}, \tilde{v}, \tilde{w})$ and of density $\tilde{\rho}$, noted temporarily by a $\tilde{\cdot}$, are defined by $\tilde{x} = \dfrac{x}{X}$. Thus, one has

$$\tilde{t} = \frac{t}{T}, \quad (\tilde{x}, \tilde{y}, \tilde{z}) = \left(\frac{x}{L}, \frac{y}{D}, \frac{z}{D}\right), \quad (\tilde{u}, \tilde{v}, \tilde{w}) = \left(\frac{u}{U}, \frac{v}{W}, \frac{w}{W}\right), \quad \tilde{\rho} = \frac{\rho}{\rho_0}\ .$$

We finally define the modified friction factor C_f/U that we write C_f.

We introduce the non-dimensional numbers:

F_r	Froude number following the Ω-plane	:	$F_r = \dfrac{U}{\sqrt{gD}}$,
F_L	Froude number following the **i**-direction	:	$F_L = \dfrac{U}{\sqrt{gL}}$,
R_μ	Reynolds numbers with respect to μ	:	$R_\mu = \dfrac{\rho_0 U L}{\mu}$,
R_λ	Reynolds numbers with respect to λ	:	$R_\lambda = \dfrac{\rho_0 U L}{\lambda}$,
M_a	Mach number	:	$M_a = \dfrac{U}{c}$,
C	Oser number	:	$C = \dfrac{M_a}{F_r} = \dfrac{\sqrt{gD}}{c}$

where the dimensionless number C is often referred as the Oser number. It determines whether the gravity should have an influence or not in the model. Let us note that the Oser number may have influence for law temperature model. In such cases, the gravity effect can be considerable (we refer to Section 4.1 for numerical illustration).

Remark 3.1. In view of Remark 2.4, in practice, the Oser number is $C \approx \dfrac{1}{1000}$. Thus, this parameter indicates that the fluid is slightly influenced by the effects of the gravity in the present modeling problem.

Dropping the $\tilde{\cdot}$, the non-dimensional compressible Navier-Stokes system becomes:

$$\left\{\begin{array}{rcl} \partial_t \rho + \partial_x(\rho u) + \mathrm{div}_{y,z}(\rho \mathbf{v}) &=& 0\ , \\ \partial_t(\rho u) + \partial_x(\rho u^2) + \mathrm{div}_{y,z}(\rho u \mathbf{v}) + \partial_x \dfrac{\rho}{M_a^2} &=& G_{\rho u}\ , \\ \varepsilon^2\left(\partial_t(\rho \mathbf{v}) + \partial_x(\rho u \mathbf{v}) + \mathrm{div}_{y,z}(\rho \mathbf{v} \otimes \mathbf{v})\right) + \nabla_{y,z} \dfrac{\rho}{M_a^2} &=& G_{\rho \mathbf{v}}\ , \end{array}\right. \tag{8}$$

where the source terms are

$$\begin{aligned} G_{\rho u} &= -\rho\frac{\sin\theta(x)}{F_L^2} + \partial_x\left(2R_\mu^{-1}\partial_x u + R_\lambda^{-1}\mathrm{div}(\mathbf{u})\right) + \mathrm{div}_{y,z}\left(\frac{R_\varepsilon(\mathbf{u})}{\varepsilon}\right) , \\ G_{\rho\mathbf{v}} &= \begin{pmatrix} 0 \\ -\dfrac{\rho\cos\theta(x)}{F_r^2} \end{pmatrix} + \partial_x\left(\varepsilon R_\varepsilon(\mathbf{u})\right) + \mathrm{div}_{y,z}\left(R_\lambda^{-1}\mathrm{div}(\mathbf{u}) + 2R_\mu^{-1}D_{y,z}(\mathbf{v})\right) , \end{aligned}$$

with the notations

$$\mathrm{div}_{y,z}U = \partial_y U + \partial_z U, \quad \mathrm{div}U = \partial_x U + \mathrm{div}_{y,z}U \quad \text{and} \quad R_\varepsilon(\mathbf{u}) = R_\mu^{-1}\left(\frac{1}{\varepsilon}\nabla_{y,z}u + \varepsilon\partial_x\mathbf{v}\right) .$$

The non-dimensional boundary conditions (5)-(6) are:

$$R_\varepsilon(\mathbf{u})\cdot\mathbf{n}\ (\mathbf{n}\cdot\mathbf{n} - \varepsilon^2(\partial_x\varphi)^2) + 2\varepsilon R_\mu^{-1}\partial_x\varphi\left(D_{y,z}(\mathbf{v})\mathbf{n}\cdot\mathbf{n} - \partial_x u\ (\mathbf{n}\cdot\mathbf{n})\right) = \left(\mathbf{n}\cdot\mathbf{n} + \varepsilon^2(\partial_x\varphi)^2\right)^{3/2}\rho\frac{k(u)}{U}u , \quad (9)$$

$$2\varepsilon^2 R_\mu^{-1}\partial_x\varphi^2\left(D_{y,z}(\mathbf{v})\mathbf{n} - \mathbf{n}\right) + \partial_x\varphi R_\varepsilon(\mathbf{u})\ (\mathbf{n}\cdot\mathbf{n} - \varepsilon^2(\partial_x\varphi)^2) = \varepsilon\left(\mathbf{n}\cdot\mathbf{n} + \varepsilon^2(\partial_x\varphi)^2\right)^{3/2}\rho\frac{k(\mathbf{v})}{U}\mathbf{v} \quad (10)$$

while the no-penetration condition (7) is not modified in its dimensionless form.

The unit outward normal vector is now

$$n_b = \frac{1}{\sqrt{\mathbf{n}\cdot\mathbf{n} + \varepsilon^2\partial_x\varphi}}\begin{pmatrix} -\varepsilon\partial_x\varphi \\ \mathbf{n} \end{pmatrix} .$$

To go further in the derivation of the pressurized model, we rearrange the terms with respect to ε to bring out the so-called hydrostatic approximation of System (8):

$$\partial_t\rho + \partial_x(\rho u) + \mathrm{div}_{y,z}(\rho\mathbf{v}) = 0 , \quad (11)$$

$$\partial_t(\rho u) + \partial_x(\rho u^2) + \mathrm{div}_{y,z}(\rho u\mathbf{v}) + \frac{1}{M_a^2}\partial_x\rho = -\rho\frac{\sin\theta(x)}{F_L^2} + \mathrm{div}_{y,z}\left(\frac{R_\mu^{-1}}{\varepsilon^2}\nabla_{y,z}u\right) + R_{\varepsilon,1}(\mathbf{u}) , \quad (12)$$

$$\frac{1}{M_a^2}\nabla_{y,z}\rho = \begin{pmatrix} 0 \\ -\dfrac{\rho\cos\theta(x)}{F_r^2} \end{pmatrix} + R_{\varepsilon,2}(\mathbf{u}) , \quad (13)$$

where the source terms are written

$$R_{\varepsilon,1}(\mathbf{u}) = R_\mu^{-1}\left(\partial_x\left(2\partial_x u + \frac{R_\lambda^{-1}}{R_\mu^{-1}}\mathrm{div}(\mathbf{u})\right) + \mathrm{div}_{y,z}\left(\partial_x\mathbf{v}\right)\right) = O(R_\mu^{-1}) ,$$

assuming that R_λ is of the same order of R_μ as said before, and

$$\begin{aligned} R_{\varepsilon,2}(\mathbf{u}) &= R_\mu^{-1}\left(\partial_x\left(\nabla_{y,z}u + \varepsilon^2\partial_x\mathbf{v}\right) + \mathrm{div}_{y,z}\left(\frac{R_\lambda^{-1}}{R_\mu^{-1}}\mathrm{div}(\mathbf{u}) + 2D_{y,z}(\mathbf{v})\right)\right) \\ &\quad -\varepsilon^2\left(\partial_t(\rho\mathbf{v}) + \partial_x(\rho u\mathbf{v}) + \mathrm{div}_{y,z}(\rho\mathbf{v}\otimes\mathbf{v})\right) \\ &= R_\mu^{-1}\left(\partial_x\left(\nabla_{y,z}u\right) + \mathrm{div}_{y,z}\left(\frac{R_\lambda^{-1}}{R_\mu^{-1}}\mathrm{div}(\mathbf{u}) + 2D_{y,z}(\mathbf{v})\right)\right) + \boldsymbol{O}(\varepsilon^2) \\ &= \boldsymbol{O}(R_\mu^{-1}) + \boldsymbol{O}(\varepsilon^2) . \end{aligned}$$

The first component of the wall-law boundary condition (9) becomes:

$$\begin{aligned} \frac{R_\mu^{-1}}{\varepsilon}\nabla_{y,z}u\cdot\mathbf{n} &= \frac{\left(\mathbf{n}\cdot\mathbf{n} + \varepsilon^2(\partial_x\varphi)^2\right)^{3/2}\rho\frac{k(u)}{U}u}{(\mathbf{n}\cdot\mathbf{n} - \varepsilon^2(\partial_x\varphi)^2)} - \varepsilon R_\mu^{-1}\left(\frac{2\partial_x\varphi\left(D_{y,z}(\mathbf{v})\mathbf{n}\cdot\mathbf{n} - \partial_x u\ (\mathbf{n}\cdot\mathbf{n})\right)}{(\mathbf{n}\cdot\mathbf{n} - \varepsilon^2(\partial_x\varphi)^2)} + \partial_x\mathbf{v}\cdot\mathbf{n}\right) \\ &= \rho\sqrt{\mathbf{n}\cdot\mathbf{n}}\frac{k(u)}{U}u + O(\varepsilon^2) + O(\varepsilon R_\mu^{-1}) \\ &= \rho K(u) + O(\varepsilon^2) + O(\varepsilon R_\mu^{-1}) . \end{aligned} \quad (14)$$

where we make use of the notations

$$K(u) = \sqrt{\mathbf{n}\cdot\mathbf{n}}\frac{k(u)}{U}u \quad \text{and} \quad \nabla_{y,z}u\cdot\mathbf{n} := \partial_{\mathbf{n}}u$$

which are respectively the friction term and the normal derivative of u in the Ω-plane.

In the same way, one can write the condition (10) as follows:

$$\begin{aligned} R_\mu^{-1}\nabla_{y,z}u &= \frac{\varepsilon^2\left(\mathbf{n}\cdot\mathbf{n}+\varepsilon^2(\partial_x\varphi)^2\right)^{3/2}\rho\frac{k(\mathbf{v})}{U}\mathbf{v}}{\partial_x\varphi(\mathbf{n}\cdot\mathbf{n}-\varepsilon^2(\partial_x\varphi)^2)} - \frac{2\varepsilon^3R_\mu^{-1}\partial_x\varphi^2\left(D_{y,z}(\mathbf{v})\mathbf{n}-\mathbf{n}\right)}{\partial_x\varphi(\mathbf{n}\cdot\mathbf{n}-\varepsilon^2(\partial_x\varphi)^2)} - \varepsilon^2\partial_x\mathbf{v}\cdot\mathbf{n} \\ &= \boldsymbol{O}(\varepsilon^2)+\boldsymbol{O}(\varepsilon^3R_\mu^{-1})\ . \end{aligned} \tag{15}$$

Whenever the relative roughness is smaller than the characteristic height of the viscous boundary layer, one can always assume the friction factor as a linear function of the Reynolds number R_e. In a general way, under physical considerations (see Section 2.3) and geometrical properties of the pipe (see for instance [26, 22, 28]), one can always assume that $C_f = \dfrac{C_0}{R_e}$ for some function C_0 depending on the material. Moreover, keeping in mind that the volume viscosity is of same order of the dynamic viscosity as said above, we shall assume the following asymptotic regime

$$R_\lambda^{-1} = \varepsilon\lambda_0, \quad R_\mu^{-1} = \varepsilon\mu_0, \quad K = \varepsilon K_0\ . \tag{16}$$

3.2 First order approximation

Assuming thin-layer assumptions, the nearly unidirectional flow induces small vertical accelerations that the Archimedes principle is applicable. As a consequence, one can drop all terms of order $O(\varepsilon^2)$ in equations (11)–(13). Moreover, in view of the asymptotic assumption (16), taking the formal limit as ε vanishes, we deduce the hydrostatic approximation

$$\partial_t\rho_\varepsilon + \partial_x(\rho_\varepsilon u_\varepsilon) + \mathrm{div}_{y,z}(\rho_\varepsilon\boldsymbol{v}_\varepsilon) = 0 \tag{17}$$

$$\partial_t(\rho_\varepsilon u_\varepsilon) + \partial_x(\rho_\varepsilon u_\varepsilon^2) + \mathrm{div}_{y,z}(\rho_\varepsilon u_\varepsilon\boldsymbol{v}_\varepsilon) + \frac{1}{M_a^2}\partial_x\rho_\varepsilon = -\rho_\varepsilon\frac{\sin\theta(x)}{F_L^2} + \mathrm{div}_{y,z}\left(\frac{\mu_0}{\varepsilon}\nabla_{y,z}u_\varepsilon\right) + O(\varepsilon) \tag{18}$$

$$\frac{1}{M_a^2}\nabla_{y,z}\rho_\varepsilon = \begin{pmatrix}0\\ -\dfrac{\rho_\varepsilon\cos\theta(x)}{F_r^2}\end{pmatrix} + \boldsymbol{O}(\varepsilon) \tag{19}$$

Let us emphasize that even if this system results from a formal limit of Equations (11)–(13) as ε goes to 0, we note its solution $(\rho_\varepsilon, u_\varepsilon, \boldsymbol{v}_\varepsilon)$ due to the explicit dependency on ε. Indeed, notice that we cannot neglect the terms $\dfrac{1}{\varepsilon}$ in Equation (18) since we are interested in computing a result at zeroth order.

Keeping in mind the above remark, the boundary conditions (14) and (15) become

$$\frac{\mu_0}{\varepsilon}\nabla_{y,z}u_\varepsilon\cdot\mathbf{n} = \rho_\varepsilon K_0(u)+O(\varepsilon) \quad \text{and} \quad \mu_0\nabla_{y,z}u_\varepsilon = \boldsymbol{O}(\varepsilon), \quad x\in(0,L),\ (y,z)\in\partial\Omega(x)\ . \tag{20}$$

Thus, from (18) and (20), the so-called "motion by slices" is obtained by solving the Neumann problem for $x\in(0,L)$

$$\left\{\begin{array}{lll} \mathrm{div}_{y,z}\left(\dfrac{\mu_0}{\varepsilon}\nabla_{y,z}u_\varepsilon\right) &=& O(\varepsilon)\ ,\quad (y,z)\in\Omega(x) \\ \mu_0\partial_{\mathbf{n}}u_\varepsilon &=& O(\varepsilon)\ ,\quad (y,z)\in\partial\Omega(x) \end{array}\right.\ .$$

Thus, we get at first order

$$u_\varepsilon(t,x,y,z) = \overline{u_\varepsilon}(t,x)$$

since

$$u_\varepsilon(t,x,y,z) = \overline{u_\varepsilon}(t,x)+O(\varepsilon)\ . \tag{21}$$

Consequently, at first order, we get

$$\overline{u_\varepsilon^2} = \overline{u_\varepsilon}^2 \ . \tag{22}$$

Moreover, from Equations (19), we obtain at first order

$$\rho_\varepsilon(t,x,y,z) \quad = \quad \xi_\varepsilon(t,x)\exp\left(-C^2\cos\theta(x)z\right)$$

for some positive function ξ_ε since

$$\rho_\varepsilon(t,x,y,z) = \xi_\varepsilon(t,x)\exp\left(-C^2\cos\theta(x)z\right) + O(\varepsilon) \ . \tag{23}$$

Noting,

$$\Psi(x) = \int_{\Omega(x)} \exp(-C^2\cos\theta(x)z)\ dy\ dz = \int_{-R(x)}^{R(x)} \exp(-C^2\cos\theta(x)z)\sigma(x,z)\,dz \ ,$$

one can therefore write at first order

$$\overline{\rho_\varepsilon u_\varepsilon} = \frac{1}{S}\int_\Omega u_\varepsilon\rho_\varepsilon\ dydz = \overline{u_\varepsilon}\frac{\xi_\varepsilon\Psi}{S} = \overline{\rho_\varepsilon}\ \overline{u_\varepsilon}$$

and deduce

$$\overline{\rho_\varepsilon u_\varepsilon^2} = \overline{\rho_\varepsilon}\ \overline{u_\varepsilon}^2 \tag{24}$$

since

$$\overline{\rho_\varepsilon}(t,x) = \frac{\xi_\varepsilon(t,x)\Psi(x)}{S(x)} \ . \tag{25}$$

In these equations $S(x)$ stands for the physical section of water

$$S(x) = \int_{\Omega(t,x)} dydz = \int_{-R(x)}^{R(x)} \sigma(x,z)\,dz \ .$$

Remark 3.2. At first order, one can deduce the vector $\boldsymbol{v}_\varepsilon$ from Equation (17).

Remark 3.3. Let us note that one of the key point in the derivation of the pressurized model is the stratified structure of the density. Following Remark 2.3, dropping all terms of order ε and setting $R_\mu^{-1} = O(\varepsilon^2)$, Ersoy *et al* [14, 13] obtained a two dimensional viscous "hydrostatic approximation", called compressible primitive equations, which is very close to the equation (17)–(19). Let us emphasize that the stratified structure was already used as a key point in the proof of an existence and a stability result in the context of atmosphere modeling.

3.3 The pressurized model

Let us first recall that $\mathbf{m} = (y, \varphi(x,y)) \in \partial\Omega(x)$ stands for the vector $\omega\mathbf{m}$ and $\mathbf{n} = \dfrac{\mathbf{m}}{|\mathbf{m}|}$ for the outward unit normal vector to the boundary $\partial\Omega(x)$ at the point $\mathbf{m}$ in the Ω-plane (as displayed on figure 1(b)).

Then, dropping all terms of order $O(\varepsilon)$ and integrating Equations (17)–(19) over the cross-section Ω, we obtain

$$\left\{\begin{array}{lcl} \partial_t(\overline{\rho_\varepsilon}S) + \partial_x(\overline{\rho_\varepsilon}S\overline{u_\varepsilon}) & = & \displaystyle\int_{\partial\Omega(x)} \rho_\varepsilon\left(u_\varepsilon\partial_x\mathbf{m} - \boldsymbol{v}_\varepsilon\right)\cdot\mathbf{n}\,ds \\ \partial_t(\overline{\rho_\varepsilon}S\overline{u_\varepsilon}) + \partial_x\left(\overline{\rho_\varepsilon}S\overline{u_\varepsilon}^2 + \dfrac{1}{M_a^2}\overline{\rho_\varepsilon}S\right) & = & -\overline{\rho_\varepsilon}S\dfrac{\sin\theta(x)}{F_L^2} + \dfrac{1}{M_a^2}\overline{\rho_\varepsilon}\dfrac{d\,S}{dx} \\ & & \displaystyle + \int_{\partial\Omega(x)} \rho_\varepsilon u_\varepsilon\left(u_\varepsilon\partial_x\mathbf{m} - \mathbf{v}\right)\cdot\mathbf{n}\,ds \\ & & \displaystyle - \int_{\partial\Omega(x)} \frac{\mu_0}{\varepsilon}\nabla_{y,z}u_\varepsilon\cdot\mathbf{n}\,ds \end{array}\right. . \tag{26}$$

Next, using the no-penetration condition (7), the following boundary integrals vanish:

$$\int_{\partial\Omega(x)} \rho_\varepsilon \left(u_\varepsilon \partial_x \mathbf{m} - \boldsymbol{v}_\varepsilon\right) \cdot \mathbf{n}\, ds = \int_{\partial\Omega(x)} \rho_\varepsilon u_\varepsilon \left(u_\varepsilon \partial_x \mathbf{m} - \boldsymbol{v}_\varepsilon\right) \cdot \mathbf{n}\, ds = 0 \ .$$

Using the boundary conditions (20), the stratified structure of ρ_ε (23) and the "motion by slices" (21), the last boundary integral becomes

$$\int_{\partial\Omega(x)} \frac{\mu_0}{\varepsilon} \nabla_{y,z} u_\varepsilon \cdot \mathbf{n}\, ds = \int_{\partial\Omega(x)} \rho_\varepsilon K_0(u_\varepsilon)\ ds = S\left(\frac{\xi_\varepsilon \Psi(x)}{S}\right)\left(K_0(\overline{u_\varepsilon})\frac{\psi(x)}{\Psi(x)}\right) = \overline{\rho_\varepsilon} K(x, u_\varepsilon)$$

with

$$K(x, u_\varepsilon) = K_0(\overline{u_\varepsilon})\frac{\psi(x)}{\Psi(x)}$$

where ψ stands for the curvilinear integral of $z \to \exp(-C^2 \cos\theta(x) z)$ along $\partial\Omega(x)$.

Remark 3.4. Keeping in mind Remark 2.4, the term $\exp(-C^2 \cos\theta(x) z)$ can be approximated by 1. As a consequence the quantity ψ is nothing else than the wet perimeter of the section Ω and thus $\left(\frac{\psi(x)}{\Psi(x)}\right)^{-1}$ is the so-called hydraulic radius. This quantity was introduce by engineers as a length scale for non-circular ducts in order to use the analysis derived for the circular pipes (see for instance [26, 27]). Let us outline that this factor is naturally obtained in the derivation of the averaged model.

Finally multiplying Equations (26) by $\frac{\rho_0 D U^2}{L}$ and setting

$$A = \overline{\rho_\varepsilon} S \text{ and } Q = A\overline{u_\varepsilon}$$

which are respectively the wet area and the discharge, we obtain the pressurized model (1) including a friction term:

$$\left\{\begin{array}{rcl} \partial_t(A) + \partial_x(Q) & = & 0 \\ \partial_t(Q) + \partial_x\left(\dfrac{Q^2}{A} + c^2 A\right) & = & -gA\sin\theta(x) + c^2 \dfrac{A}{S}\dfrac{dS}{dx} - gAK(x, Q/A) \end{array}\right. . \tag{27}$$

This model takes into account the slope variation, change of section and the friction due to roughness on the inner wall of the pipe. This system was formally introduced by the author in [11] and [5] in the context of unsteady mixed flows in closed water pipes assuming the motion by slices that we have justified here.

We have proposed a Finite volume discretisation of the pressurized model introducing a new kinetic solver in [2] based on the kinetic scheme of Perthame and Simeoni [23]. We have also proposed a new well-balanced VFRoe scheme. These numerical scheme have been validated in [2] and [3] in a quasi-frictionless cone-shaped (expanding and contracting) with a numerical confrontation with the equivalent pipe method used by the engineers (see [1]) in the case of an immediate flow shut down. The case of pipe with uniform section has been also considered in a code to code comparison with the so-called `belier` code. This code is based on the method of characteristics to solve the Allievi equations. In any case, the obtained results are in a very good agreement. We also have proposed several test cases in the context of unsteady mixed flows in [7].

4 Concluding remarks

In this note, we have performed an asymptotic analysis of the 3D compressible Navier-Stokes equation with wall-law and no-penetration conditions in the thin-layer limit. We have considered the compressible hydrostatic approximation with friction boundary conditions and we have integrated these equations along the Ω sections to get the pressurized model. In particular, we have shown that the pressurized model (27)

is an approximation of $O(\varepsilon)$ of the hydrostatic approximation (17)–(19) and therefore of the compressible Navier-Stokes equations (8).

We numerically investigate the paraboloid correction on (y,z) in the expansion of $u_\varepsilon(t,x,y,z)$ and we show in particular the influence of the gravity through the Oser number. We finally end the paper by discussing the generalization of this work to gas/fluid flow governed by the Compressible Navier-Stokes equations with a barotropic pressure law

$$p(\rho) = c^2\rho^\gamma \quad \text{with } \gamma > 1$$

at low Oser.

4.1 Second order approximation

One can also formally increase the order of accuracy by determining the first order correction on (y,z) in the expansion of $u_\varepsilon(t,x,y,z)$. It corresponds to a paraboloid correction. To do so, let us come back to the equation (12) and write:

$$\begin{aligned}
\mathrm{div}_{y,z}\left(\frac{\mu_0}{\varepsilon}\nabla_{y,z}u_\varepsilon\right) &= \partial_t(\rho_\varepsilon u_\varepsilon) + \partial_x(\rho_\varepsilon u_\varepsilon^2) + \mathrm{div}_{y,z}(\rho_\varepsilon u_\varepsilon \boldsymbol{v}_\varepsilon) + \frac{1}{M_a^2}\partial_x\rho_\varepsilon + \rho_\varepsilon\frac{\sin\theta(x)}{F_L^2} + O(\varepsilon)\\
&= \rho_\varepsilon\left(\partial_t(u_\varepsilon) + \boldsymbol{u}_\varepsilon\cdot\nabla(u_\varepsilon)\right) + \frac{1}{M_a^2}\partial_x\rho_\varepsilon + \rho_\varepsilon\frac{\sin\theta(x)}{F_L^2} + O(\varepsilon)\\
&= \rho_\varepsilon\left(\partial_t(\overline{u_\varepsilon}) + \overline{u_\varepsilon}\partial_x(\overline{u_\varepsilon}) + \frac{\sin\theta(x)}{F_L^2}\right) + \frac{1}{M_a^2}\partial_x\rho_\varepsilon + O(\varepsilon)
\end{aligned}$$

We deduce from the relation (25) and the conservation of the momentum equation (27):

$$\xi_\varepsilon\left(\partial_t(\overline{u_\varepsilon}) + \overline{u_\varepsilon}\partial_x(\overline{u_\varepsilon}) + \frac{\sin\theta(x)}{F_L^2}\right) + \frac{1}{M_a^2}\partial_x\xi_\varepsilon = -\xi_\varepsilon\left(K(x,u_\varepsilon) + \frac{\partial_x\Psi(x)}{\Psi(x)}\right)\ .$$

Thus, one can obtain the paraboloid correction in the asymptotic expansion of u_ε by solving the following Poisson equation

$$-\mathrm{div}_{y,z}\left(\frac{\mu_0}{\varepsilon}\nabla_{y,z}u_\varepsilon\right) = F_{t,x}(z) + O(\varepsilon), \quad x\in(0,L), \quad (y,z)\in\Omega(x)$$

with the boundary condition

$$\mu_0\nabla_{y,z}u_\varepsilon = O(\varepsilon),\ x\in(0,L), \quad (y,z)\in\partial\Omega(x)$$

where the right hand side reads

$$F_{t,x}(z) = \xi_\varepsilon\exp(-C^2\cos\theta(x)z)\left(K(x,u_\varepsilon) + \frac{\partial_x\Psi(x)}{\Psi(x)}\right)\ .$$

Let us numerically illustrate the paraboloid correction of u_ε. In particular, let us focus on the influence of the Oser number $C = \dfrac{M_a}{F_r}$. We consider three type of geometry (section): circular, rectangular and "horseshoe" (see figure 2). We consider the following settings

$$\varepsilon = 10^{-3}, \quad \overline{u_\varepsilon} = 0, \quad \cos\theta = 1 \quad \text{and} \quad \xi_\varepsilon\left(K(x,u_\varepsilon) + \frac{\partial_x\Psi(x)}{\Psi(x)}\right) = 1.$$

Then we compute the numerical solution of the Poisson equation by fixing the Oser number to $C=1$ and $C=10^{-3}$ for each type of geometry.

The first test case $C=1$ represents the situation when the gravity effects are important while in the second one we neglect its influence. The gravity may have a non negligible contribution under thermodynamical

considerations. For instance, the more the fluid is compressible and the more the sound speed decay c, i.e. C becomes large, as in two phase flows.

The results are obtained on figures 3(a), 4(a) and 5(a) for the case $C = 1$ and on figures 3(b), 4(b) and 5(b) for the second test case.

Whenever the effects of gravity are small, the center of the paraboloid profile of the velocity u_ε is localized at the main pipe axis. This behavior is lost when the influence of gravity becomes important. One can observe these statements for each type of sections: circular on figure 3, rectangular on figure 4 and "horseshoe" 5.

Let us also add that the scale of the paraboloid is of order ε as predicted by the asymptotic expansion of u_ε, in particular the expression (21).

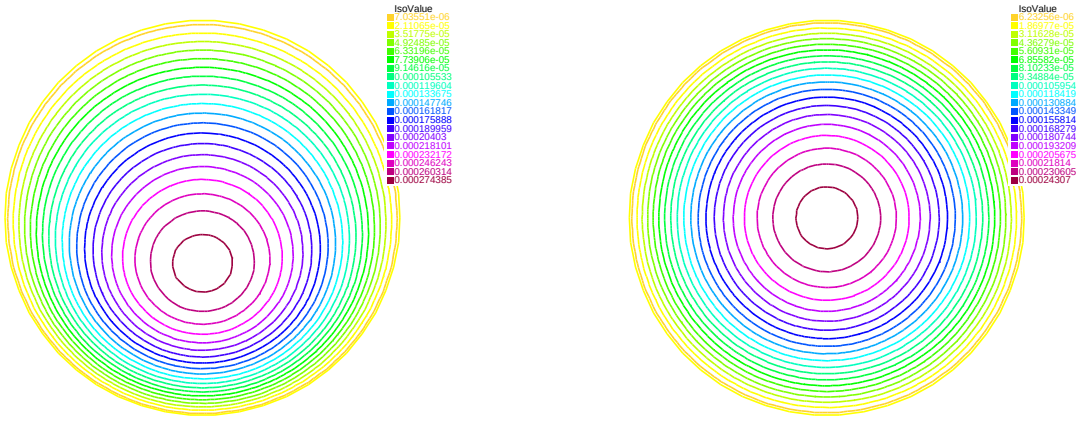

(a) $C = 1$ (b) $C \ll 1$

Figure 3: Circular section

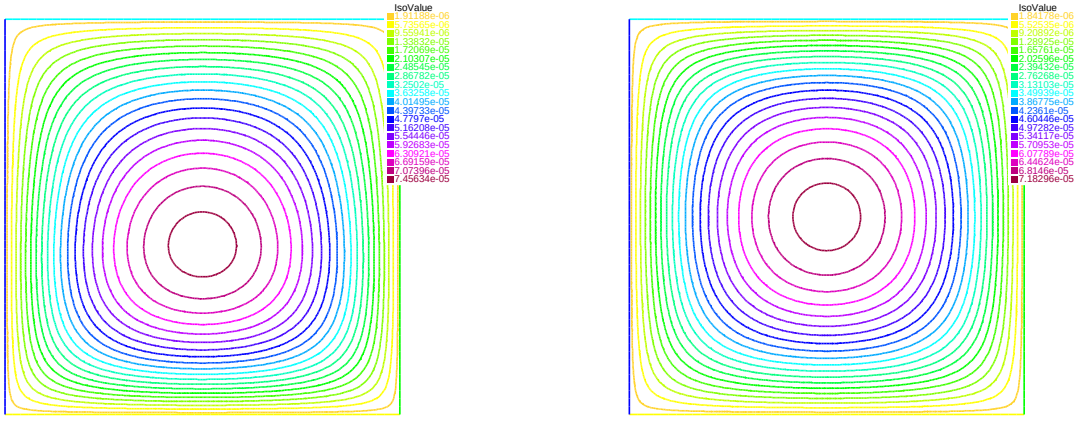

(a) $C = 1$ (b) $C \ll 1$

Figure 4: Rectangular section

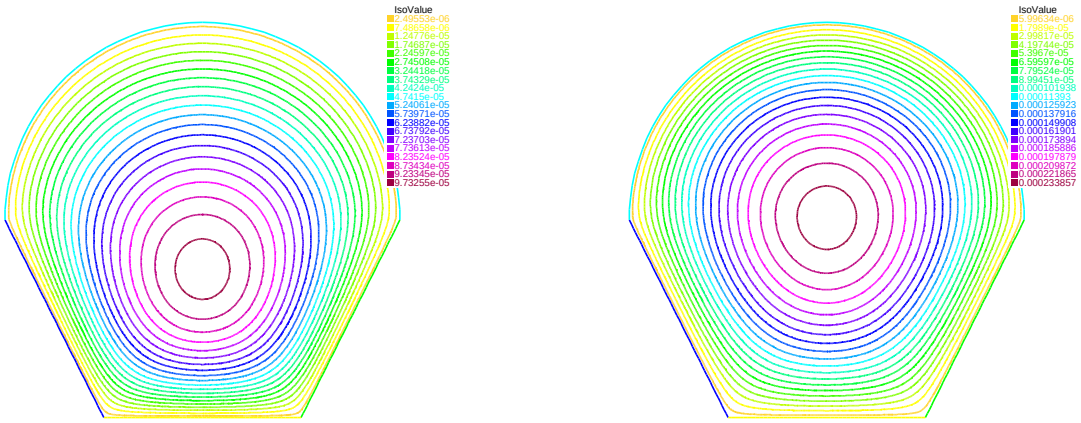

(a) $C = 1$ (b) $C \ll 1$

Figure 5: "horseshoe" section

4.2 Averaged Low Oser compressible models

Neglecting the influence of the gravity, the author consider in [6] the air entrainment appearing in the transient flow in closed pipes filled by the "free surface" flow and air flow. The free surface model is obtained in a very closed manner as the derivation of Saint-Venant equations for free surface open channel flows (see [12]). The air flow is assumed to be governed by the 3D compressible Euler equations with $p(\rho) = c^2\rho^\gamma$, $\gamma = \dfrac{7}{5}$. Under the assumptions

$$\overline{u^2} \approx \overline{u}^2 \quad \text{and} \quad \overline{\rho^\gamma} \approx \overline{\rho}^\gamma \ ,$$

taking the averaged values over cross-sections of the main flow axis, they obtained a system of four partial differential equations.

Let us outline that this assumption

$$\overline{\rho^\gamma} \approx \overline{\rho}^\gamma$$

is obviously true when the gravity has no influence in the model. Nevertheless, it becomes generally wrong when the fluid/gas flow is influenced by the gravity.

Thus, we aim to provide a physical and mathematical background such that this assumption still holds when the gravity plays a role. This will allows to derive averaged models of Equations (2) with a general pressure law $p(\rho) = c^2\rho^\gamma$ with $\gamma > 1$ in a thin-layer framework. We want to generalize the air layer model introduced in [6] to gas/fluid flow which can be influenced by the effects of gravity.

Let us emphasize that the derivation of the air layer model is based on the **P**-model [5] and thus the proposed derivation (Sections 2 and 3) can be applied. It suffices to replace in all previous equations the pressure law $p(\rho) = c^2\rho$ by $p(\rho) = c^2\rho^\gamma$ with $\gamma > 1$.

Thus in the hydrostatic approximation, in particular Equation (19), the density, at first order, is now

$$\rho_\varepsilon(t,x,y,z) = \xi_\varepsilon(t,x)N(t,x,z)$$

where

$$N(t,x,z) = \left(1 + zC^2\cos\theta(x)\frac{1-\gamma}{\gamma\xi_\varepsilon(t,x)^{\gamma-1}}\right)^{\frac{1}{\gamma-1}}$$

for some function ξ_ε.

Then, the "motion by slices" (21) as well as the relation (22) still hold and at first order one has

$$\overline{\rho_\varepsilon u_\varepsilon} = \frac{1}{S}\int_\Omega u_\varepsilon\rho_\varepsilon \ dydz = \overline{\rho_\varepsilon u_\varepsilon}, \quad \text{and} \quad \overline{\rho_\varepsilon u_\varepsilon^2} = \overline{\rho_\varepsilon}\ \overline{u_\varepsilon}^2$$

since

$$\overline{\rho_\varepsilon}(t,x) = \xi_\varepsilon(t,x)\overline{N}(t,x)$$

where

$$\overline{N}(t,x) = \frac{1}{S(x)}\int_{\Omega(x)} N(t,x,z)\; dy\; dz\;.$$

To go further in the derivation, if we integrate ρ^γ along a section Ω we found that, even in the case $\gamma = 2$, at first order,

$$\overline{\rho_\varepsilon}^{\gamma} \not\simeq \overline{\rho_\varepsilon^\gamma}$$

Following Section 3 and keeping $\overline{\rho^\gamma}$, the resulting averaged model is

$$\left\{\begin{array}{lcl} \partial_t(\overline{\rho_\varepsilon}S) + \partial_x(\overline{\rho_\varepsilon}S\overline{u_\varepsilon}) & = & 0 \\ \partial_t(\overline{\rho_\varepsilon}S\overline{u_\varepsilon}) + \partial_x\left(\overline{\rho_\varepsilon}S\overline{u_\varepsilon}^2 + \dfrac{1}{M_a^2}\overline{\rho_\varepsilon^\gamma}S\right) & = & -\overline{\rho_\varepsilon}S\dfrac{\sin\theta(x)}{F_L^2} + \dfrac{1}{M_a^2}\overline{\rho_\varepsilon^\gamma}\dfrac{d\,S}{dx} - \overline{\rho_\varepsilon}K(x,\overline{u_\varepsilon}) \end{array}\right. . \tag{28}$$

This model is useless since it is *a priori* ill-posed due to the term $\overline{\rho_\varepsilon^\gamma}$ which cannot be determined from $\overline{\rho_\varepsilon}$. To make it usable one has to add an extra assumption in the asymptotic assumptions (16) concerning the Oser number. Namely, if we assume that

$$C = O(\varepsilon^p) \quad \text{with } p \geqslant \frac{1}{2}\;,$$

then, one has

$$N(t,x,z) = 1 + O(C^2) = 1 + O(\varepsilon^{2p})\;.$$

Thus, the density is now approximated by

$$\overline{\rho_\varepsilon} = \xi_\varepsilon + O(C^2) = \xi_\varepsilon + O(\varepsilon^{2p})$$

and we finally deduce

$$\overline{\rho_\varepsilon^\gamma} = \xi_\varepsilon^\gamma + O(C^2) = \xi_\varepsilon^\gamma + O(\varepsilon^{2p})$$

Thus, we obtain a class of averaged low Oser compressible models with $\gamma > 1$:

$$\left\{\begin{array}{lcl} \partial_t(\xi_\varepsilon S) + \partial_x(\xi_\varepsilon S\overline{u}) & = & 0 \\ \partial_t(\xi_\varepsilon S\overline{u_\varepsilon}) + \partial_x\left(\xi_\varepsilon S\overline{u_\varepsilon}^2 + \dfrac{1}{M_a^2}\xi_\varepsilon^\gamma S\right) & = & -\xi_\varepsilon S\dfrac{\sin\theta(x)}{F_L^2} + \dfrac{1}{M_a^2}\xi_\varepsilon^\gamma\dfrac{d\,S}{dx} - \xi_\varepsilon K(x,\overline{u_\varepsilon}) \end{array}\right. \tag{29}$$

as an approximation of order $O(\varepsilon)$ of the Compressible Navier-Stokes equation (8) with wall-law and no-penetration boundary conditions. One can also consider the model (29) as an approximation of order $O(C^2)$ of the model (28). In view of Remark 3.1, let us note that this result also holds for $\gamma = 1$.

References

[1] A. Adamkowski, *Analysis of transient flow in pipes with expanding or contracting sections*, ASME J. of Fluid Engineering, 125 (2003), pp. 716–722.

[2] C. Bourdarias, M. Ersoy, and S. Gerbi, *A kinetic scheme for pressurised flows in non uniform closed water pipes*, in Maths and water, Monogr. Real Acad. Ci. Exact. Fís.-Quím. Nat. Zaragoza, 31, Real Acad. Ci. Exact., Fís. Quím. Nat. Zar, Zaragoza, 2009, pp. 1–20.

[3] ———, *A model for unsteady mixed flows in non uniform closed water pipes and a well-balanced finite volume scheme*, Int. J. Finite Vol., 6 (2009), p. 47.

[4] ——, *A kinetic scheme for transient mixed flows in non uniform closed pipes: a global manner to upwind all the source terms*, J. Sci. Comput., 48 (2011), pp. 89–104.

[5] ——, *A mathematical model for unsteady mixed flows in closed water pipes*, Sci. China Math., 55 (2012), pp. 221–244.

[6] ——, *Air entrainment in transient flows in closed water pipes: a two-layer approach*, ESAIM Math. Model. Numer. Anal., 47 (2013), pp. 507–538.

[7] ——, *A model for unsteady mixed flows in non uniform closed water pipes: a Full Kinetic Approach*, Accepted in Numer. Math., (2014), p. 40.

[8] C. Bourdarias and S. Gerbi, *A finite volume scheme for a model coupling free surface and pressurised flows in pipes*, J. Comp. Appl. Math., 209 (2007), pp. 109–131.

[9] H. Capart, X. Sillen, and Y. Zech, *Numerical and experimental water transients in sewer pipes*, Journal of Hydraulic Research, 35 (1997), pp. 659–672.

[10] N. T. Dong, *Sur une méthode numérique de calcul des écoulements non permanents soit à surface libre, soit en charge, soit partiellement à surface libre et partiellement en charge*, La Houille Blanche, 2 (1990), pp. 149–158.

[11] M. Ersoy, *Modélisation, analyse mathématique et numérique de divers écoulements compressibles ou incompressibles en couche mince*, PhD thesis, Université de Savoie, 2010. available at http://tel.archives-ouvertes.fr/tel-00529392.

[12] ——, *A free surface model for incompressible pipe and open channel flow*, (2013).

[13] M. Ersoy and T. Ngom, *Existence of a global weak solution to compressible primitive equations*, C. R. Math. Acad. Sci. Paris, 350 (2012), pp. 379–382.

[14] M. Ersoy, T. Ngom, and M. Sy, *Compressible primitive equations: formal derivation and stability of weak solutions*, Nonlinearity, 24 (2011), pp. 79–96.

[15] S. Ferrari and F. Saleri, *A new two-dimensional shallow water model including pressure effects and slow varying bottom topography*, M2AN Math. Model. Numer. Anal., 38 (2004), pp. 211–234.

[16] M. Fuamba, *Contribution on transient flow modelling in storm sewers*, Journal of Hydraulic Research, 40 (2002), pp. 685–693.

[17] J.-F. Gerbeau and B. Perthame, *Derivation of viscous Saint-Venant system for laminar shallow water; numerical validation*, Discrete Cont. Dyn. Syst. Ser. B, 1 (2001), pp. 89–102.

[18] M. Hamam and A. McCorquodale, *Transient conditions in the transition from gravity to surcharged sewer flow*, Can. J. Civ. Eng., 9 (1982), pp. 189–196.

[19] N. E. Kochin, *On simplification of the equations of hydromechanics in the case of the general circulation of the atmosphere*, Trudy Glavn. Geofiz. Observator., 4 (1936), pp. 21–45.

[20] L. D. Landau and E. M. Lifshitz, *Fluid mechanics*, Translated from the Russian by J. B. Sykes and W. H. Reid. Course of Theoretical Physics, Vol. 6, Pergamon Press, London, 1959.

[21] F. Marche, *Derivation of a new two-dimensional viscous shallow water model with varying topography, bottom friction and capillary effects*, European Journal of Mechanic. B, Fluids, 26 (2007), pp. 49–63.

[22] P. H. Oosthuizen and W. E. Carscallen, *Compressible fluid flow*, McGraw-Hill, New York, 1997.

[23] B. Perthame and C. Simeoni, *A kinetic scheme for the Saint-Venant system with a source term*, Calcolo, 38 (2001), pp. 201–231.

[24] P. Roe, *Some contributions to the modelling of discontinuous flow*, in Large-scale computations in fluid mechanics. Part 2. Proceedings of the fifteenth AMS-SIAM summer seminar on applied mathematics held at Scripps Institution of Oceanography, La Jolla, Calif., June 27-July 8, 1983, B. E. Engquist, S. Osher, and R. C. J. Somerville, eds., vol. 22 of Lectures in Applied Mathematics, American Mathematical Society, 1985, pp. 163–193.

[25] C. Song, J. Cardle, and K. Leung, *Transient mixed-flow models for storm sewers*, Journal of Hydraulic Engineering, ASCE, 109 (1983), pp. 1487–1503.

[26] V. Streeter and E. Wylie, *Fluid Transients*, McGraw-Hill, New York, 1978.

[27] ——, *Fluid transients in systems*, Prentice Hall, Englewood Cliffs, NJ, 1993.

[28] V. Streeter, E. Wylie, and K. Bedford, *Fluid Mechanics*, McGraw-Hill, 1998.